ASTRONOMY & ASTROPHYSICS SUPPLEMENT SERIES

FEBRUARY I **2000**, PAGE 469

Astron. Astrophys. Suppl. Ser. **141**, 469–490 (2000)

HI observations of nearby galaxies

I. The first list of the Karachentsev catalog

W.K. Huchtmeier[1], I.D. Karachentsev[2], V.E. Karachentseva[3], and M. Ehle[4]

[1] Max-Planck-Institut für Radioastronomie, Auf dem Hügel 69, D-53121 Bonn, Germany
[2] Special Astrophysical Observatory, Russian Academy of Sciences, N. Arkhyz, KChR, 357147, Russia
[3] Astronomical Observatory of Kiev University, Kiev, Ukraine
[4] Max-Planck-Institut für Extraterrestrische Physik, Giessenbachstraße, D-85740 Garching bei München, Germany

Received September 14; accepted November 16, 1999

Abstract. We present HI observations of the galaxies in the first list of the Karachentsev catalog of previously unknown nearby dwarf galaxies (Karachentseva & Karachentsev 1998). This survey covers all known nearby galaxy groups within the Local Volume (i.e. within 10 Mpc) and their environment, that is about 25% of the total sky. A total of 257 galaxies have been observed with a detection rate of 60%. We searched a frequency band corresponding to heliocentric radial velocities from -470 km s^{-1} to $\sim$+4000 km s^{-1}. Non-detections are either due to limited coverage in radial velocity, confusion with Local HI (mainly in the velocity range -140 km s^{-1} to +20 km s^{-1}), or lack of sensitivity for very weak emission. 25% of the detected galaxies are located within the Local Volume. Those galaxies are dwarf galaxies judged by their optical linear diameter (1.4 $\pm$ 0.2 kpc on the average), their mean total HI mass (4.6 10^7 $M_\odot$), and their observed linewidths (39 km s^{-1}).

Key words: galaxies: distances and redshifts; dwarf; fundamental parameters; general

1. Introduction

The only way to study the smallest galaxies is to search for them in our cosmic neighborhood. The first systematic catalog of nearby galaxies was prepared by Kraan-Korteweg & Tammann (1979) who collected all known galaxies with corrected radial velocities v_0 $\leq$ 500 km s^{-1}, a total of 179 objects (hereafter called the KKT sample). Since that time the number of known galaxies within the Local Volume (i.e. within a distance of 10 Mpc) increased to 303 objects (Karachentsev et al. 1999). For the past decade the initial KKT sample has been increased almost two times in number due to the mass redshift surveys of galaxies from the known catalogues, revealing new nearby galaxies in the Milky Way "Zone of Avoidance", as well as special searches for dwarf galaxies in nearby groups. The increasing numbers of galaxies in the Local Volume is mainly due to many new dwarf galaxies. This fact demonstrates how incomplete our knowledge about the galaxy population of even the Local Volume is.

A couple of years ago Karachentseva & Karachentsev (1998; hereafter KK98) initiated an all-sky search for candidates for new nearby dwarf galaxies using the second Palomar Sky Survey and the ESO/SERC plates of the southern sky. The results of the first two segments of the survey have been published, they cover large areas around the known galaxy groups in the Local Volume (KK98) and the area of the Local Void (Karachentseva et al. 1999). In a next step to derive distances we will measure radial velocities. Later on we will aim for more exact photometric distances. In this paper we present the first follow-up observations, the HI search for the galaxies in KK98. The HI search for dwarf irregular galaxies seems quite efficient as these galaxies are HI rich in general and with adequate velocity resolution, say 5 km s^{-1}, all the HI of a given galaxy will be within a few velocity channels. The characteristic signature of a dwarf galaxy profile, a nearly gaussian structure, is different from radio interference and easily will lead to a good signal-to-noise ratio.

2. Observations

Observations were performed with three different radio telescopes for different declination ranges. The 100-m radiotelescope at Effelsberg was used for declinations greater

Send offprint requests to: W.K. Huchtmeier,
e-mail: huchtmeier@mpifr-bonn.mpg.de

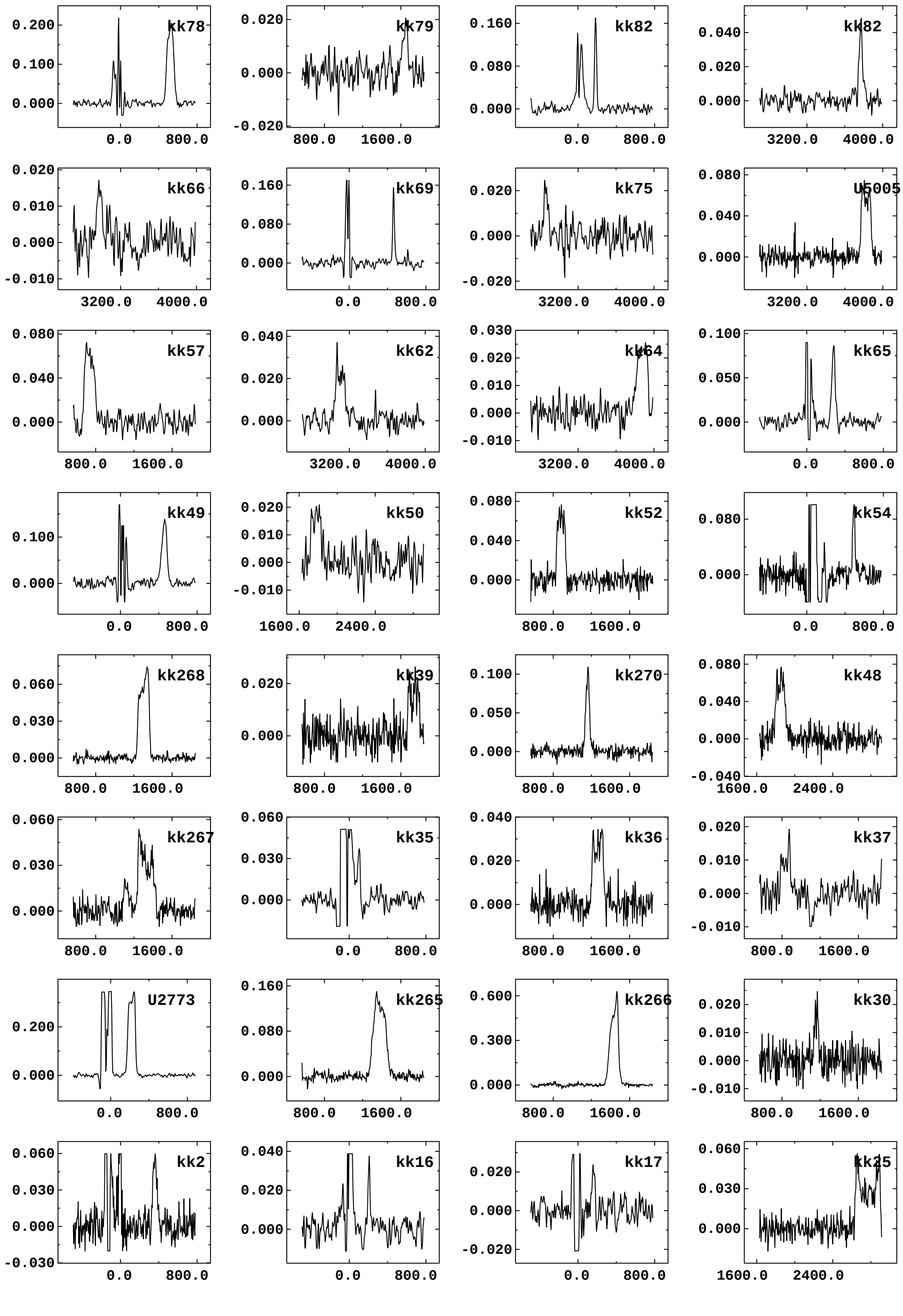

Fig. 1. HI profiles observed with the 100-m radio telescope at Effelsberg which has a HPBW of 9.′3 at a wavelength of 21 cm. Observations were obtained in the total power mode [ON – OFF] which yields a residual of the Local HI emission around 0 km s^{-1}. The profiles are arranged in ascending R.A. starting at the bottom left corner

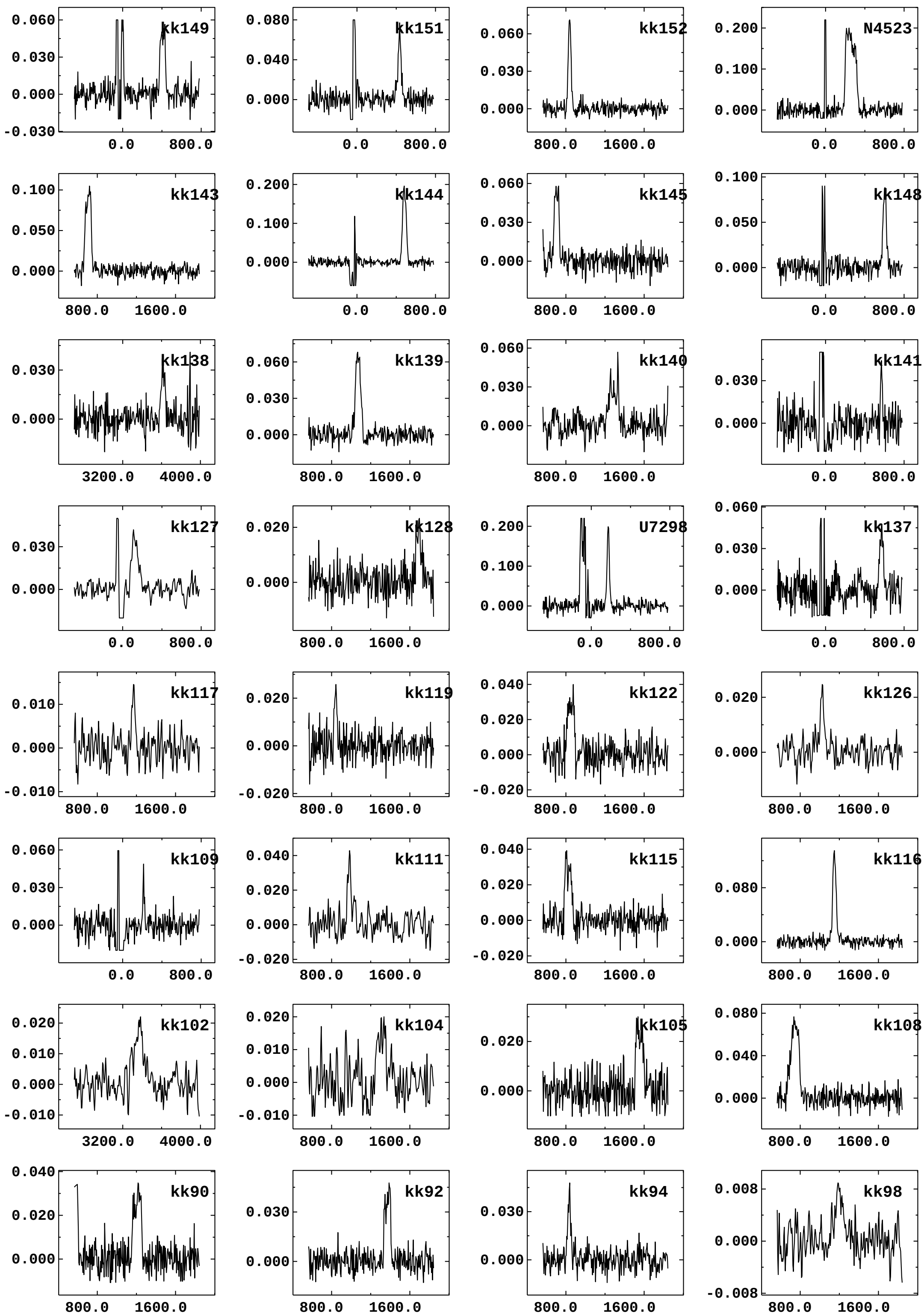

Fig. 1. continued

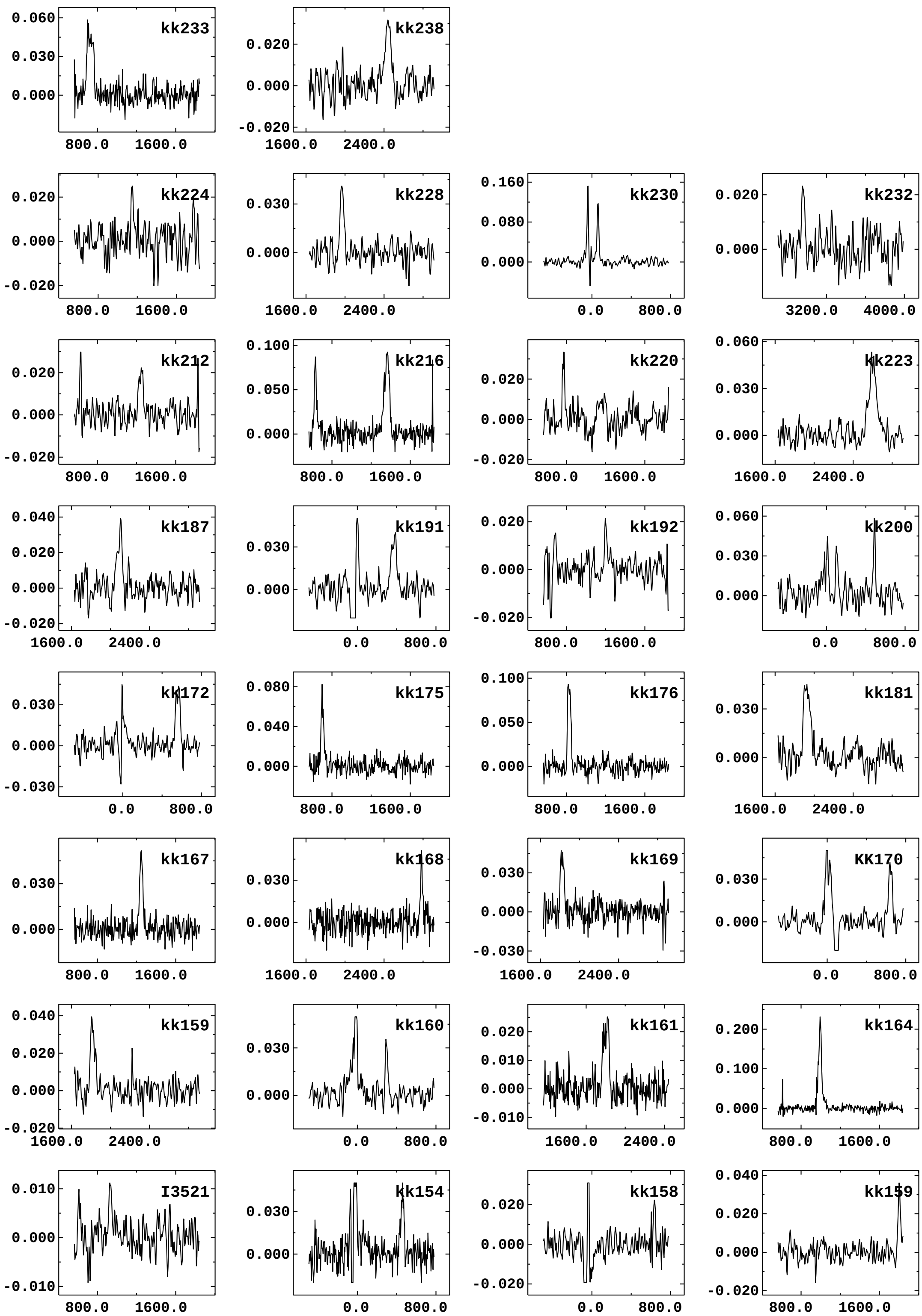

Fig. 1. continued

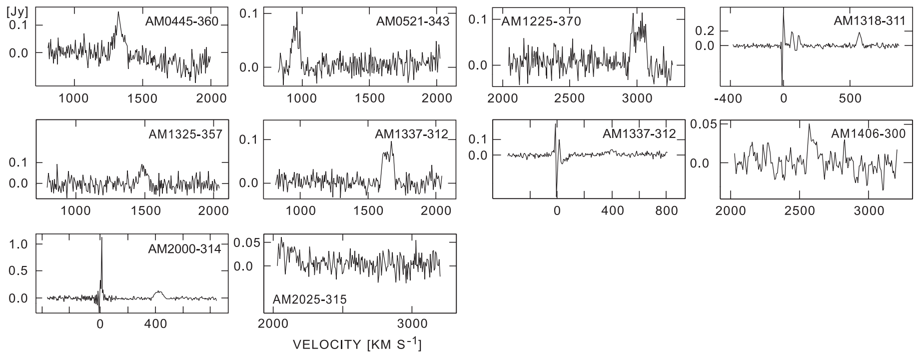

Fig. 2. HI profiles observed with the Nançay radio telescope (HPBW of $3'.6 \times 22'$ for the declination range in question)

than −31°, the Nançay radio telescope was selected for galaxies in the declination range −38° ≤ −31°, and the compact array of the Australia Telescope was used for galaxies south of −38°.

2.1. Effelsberg observations

The radio telescope at Effelsberg has been used in the total power mode (ON – OFF) combining a reference field 5 min earlier in R.A. with the on-source position. A dual channel HEMT receiver had a system noise of 30 K.

The 1024 channel autocorrelator was split into 4 bands (bandwidth 6.25 MHz) of 256 channels each shifted in frequency by 5 MHz with respect to their neighbor in order to cover a velocity range from −470 to 3970 $\mathrm{km\,s^{-1}}$ overlapping 1.5 MHz between channels. The resulting channel separation was 5.1 $\mathrm{km\,s^{-1}}$ yielding a resolution of 6.2 $\mathrm{km\,s^{-1}}$ (10.2 $\mathrm{km\,s^{-1}}$ after Hanning smoothing). The HI profiles observed with the 100-m radiotelescope are presented in Fig. 1 in order of increasing R.A. as in Table 1. The half power beam widths (HPBW) of the Effelsberg telescope at this wavelength is $9'.3$.

2.2. Nançay observations

For 15 galaxies in the declination range −38° ≤ −31° the Nançay radio telescope was used with the same velocity resolution and coverage. Major differences to the description given for the Effelsberg observations were a different system noise (45 K), a different antenna beam ($3'.6 \times 22'$ in R.A. and Dec. for this declination range), and shorter integration phases with a cycle of 2 minutes for the ON and the OFF positions. Nine galaxies have been detected (Fig. 2).

2.3. Compact Array of the Australia Telescope

40 of the 57 galaxies south of declination −38° have been observed with the Compact Array of the Australia Telescope. For this HI search we have chosen the 750A antenna array configuration in order to yield an antenna beam comparable to the optical size of the smallest galaxies (i.e. ∼ 1′). The frequency setup and correlator configuration was such that we obtained a velocity coverage from −450 to +2900 $\mathrm{km\,s^{-1}}$ and a channel separation of 6.6 $\mathrm{km\,s^{-1}}$ (i.e. a resolution of 7.9 $\mathrm{km\,s^{-1}}$). Each galaxy was observed for 10 min every few hours. With five to six observations per target position we achieved a regular coverage of the *uv* plane for these "snapshot mode" observations. The resulting integrated HI profiles are given in Fig. 3 (for a more detailed discussion of these data see Huchtmeier et al. in preparation). We may miss some flux with the interferometer (missing flux) as the observed HI emission extends over more than 2′ per channel for over 60% of the galaxies. Galaxies from the kk98 sample not observed are: kk 11, kk 63, kk179, kk 184, kk 189, kk 190, kk 197, kk 203, kk 211, kk 213, kk 214, kk 217, kk 221, kk 222, kk 235, kk 244, kk 248.

3. The data

Our search list was an early version of the list of KK98 containing a few additional galaxies which did not make it into the final version because of their morphology and/or size (i.e. they were too small). Particularly, we took into account the results of HI searches for nearby dwarf galaxies made by Kraan-Korteweg et al. (1994), Huchtmeier et al. (1995), Burton et al. (1996), Huchtmeier & van Driel (1996), Huchtmeier et al. (1997) and Cote et al. (1997). The optical data of our galaxies are given in Table 1. The kk-number (or other identification if there is no kk-number) is given in Col. 1, R.A. and Dec. (1950) follow in Cols. 2 and 3. The optical diameters a and b in the de Vaucouleurs (D_{25}) system follow in Cols. 4 and 5, the morphological type in Col. 6 where we use the following coding:

Im - irregular blue object with bright knot(s);
Ir - irregular without knots or with amorphous condensations, the colour is neutral or bluish;

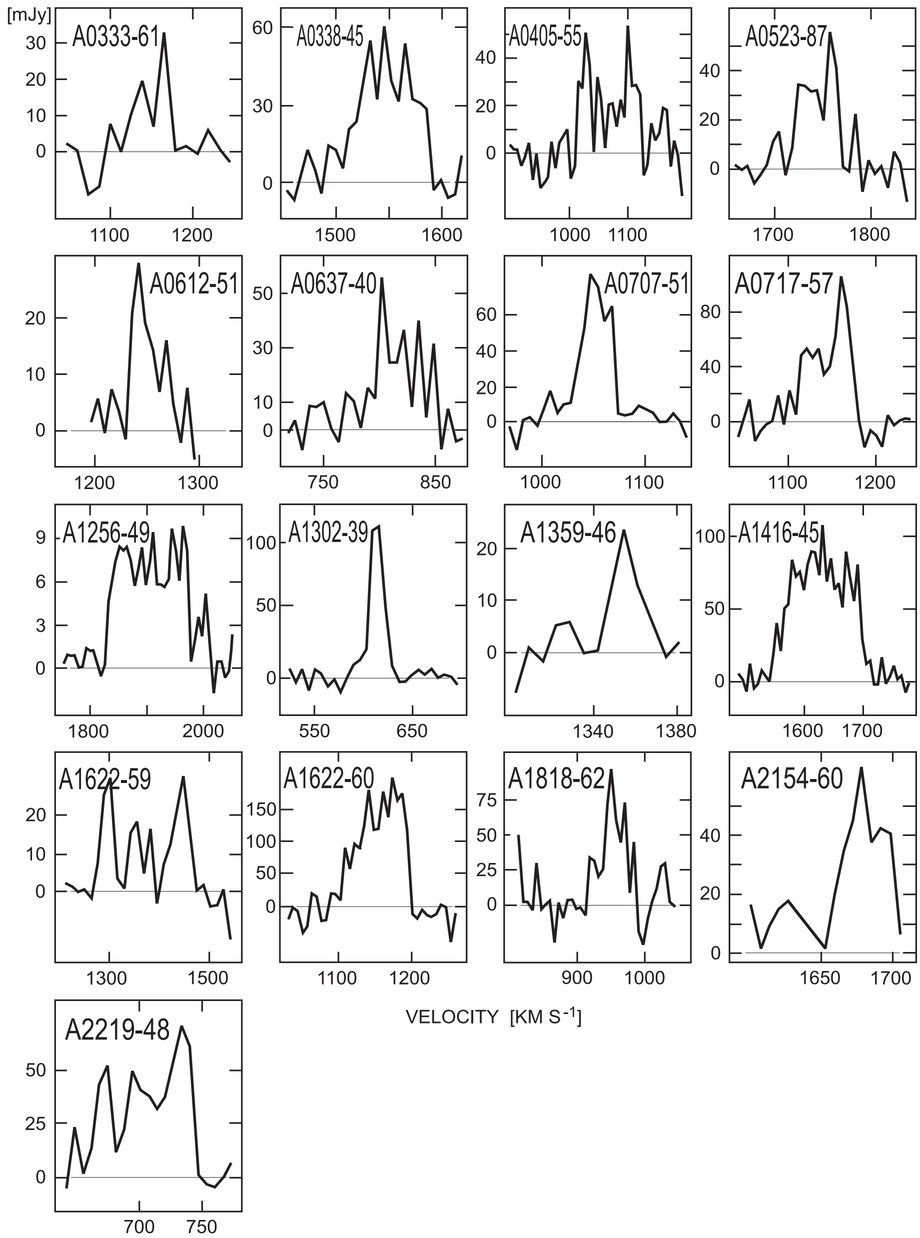

Fig. 3. HI profiles observed with the Australia Telescope Compact Array. The synthesized antenna beam is of the order of 1′

Sm - disturbed spiral or irregular with signs of spiral structure;

Sph - spheroidal, with very low brightness gradient or without any, the color is neutral or redish.

The optical surface brightness (SB) has been coded (see KK98): high (H), low (L), very low (VL), and extremely low (EL) in Col. 7. The total blue magnitude $B_{\rm t}$ and its reference follow in Cols. 8 and 9. "NED" - data are from the NASA/Extragalactic Database, "IK" - visual estimates from POSS (typical error is about 0.4 mag) by I. Karachentsev, "6 m" - accurate photometric data from the 6-m telescope CCD-frames obtained by Karachentsev and coworkers (unpublished); "UH" - photometric data from U. Hopp (Calar Alto) unpublished. The Galactic extinction follows in Col. 10. Other names (identifications) are listed in Col. 11.

Results of the HI observations are summarized in Table 2. The kk-number is given in Col. 1, the HI-flux [Jy km s^{-1}] follows in Col. 2, the maximum emission and/or the rms noise [mJy] in Col. 3, the heliocentric radial velocity plus error in Col. 4, the line widths at the 50%, the 25%, and the 20% level of the peak emission in Col. 5. Distances (Col. 6) have been derived with different methods, there are photometric distances in

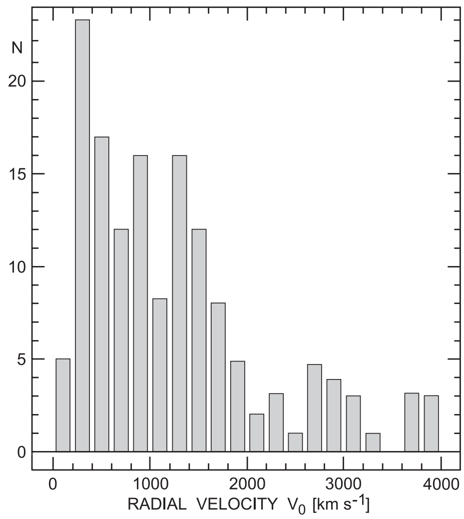

Fig. 4. The histogram shows the number of galaxies per velocity interval of 200 km s^{-1}. The distribution of corrected radial velocities (v_0) of our galaxy sample demonstrates the local character of these galaxies

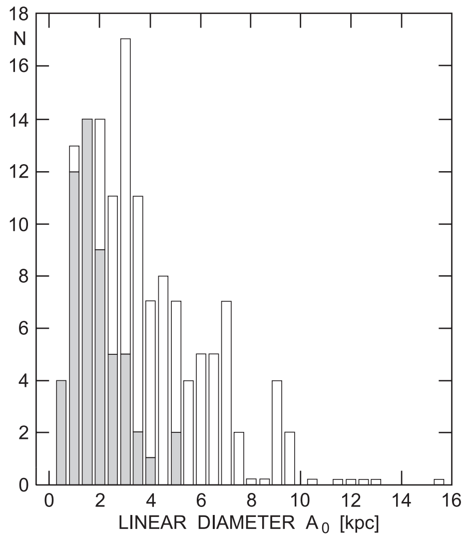

Fig. 5. The distribution of the optical linear diameter A_0 in kpc for the whole sample in the de Vaucouleurs (D_{25}) system is given here. Galaxies within 10 Mpc (i.e. within the Local Volume) are shown by shaded areas. The medium value for the shaded areas is 1.4 ± 0.2 kpc

some cases, in other cases the group membership yields a distance. If no other distance estimate is available, we assumed a Hubble constant of 75 km s^{-1} Mpc^{-1} to derive a "kinematic" distance. The absolute magnitude is given in Col. 7, the integrated HI mass (Col. 8) was calculated as (e.g. Roberts 1969)

$$(M_{\rm HI}/M_{\odot}) = 2.355\ 10^5 \times D^2 \times \int S_v {\rm d}v$$

where D is the distance of the galaxy in Mpc and $\int S_v {\rm d}v$ is the integrated HI flux in Jy km s^{-1}. The relative HI content $M_{\rm HI}/L_B$ follows in Col. 9. Finally, Col. 10 contains comments relative to the telescope used for the observation: unless otherwise noted observations have been performed with the 100-m radiotelescope at Effelsberg, N - marks the Nançay radio telescope, ATCA - the Australia Telescope Compact Array at Culgoora, NSW.

In a number of cases emission at negative radial velocities has been observed (kk 20, kk 236, kk 237; only kk 236 has been plotted as an example). The Dwingeloo HI survey (Hartmann & Burton 1997) has been consulted: in all cases of negative radial velocities extended HI emission was found suggesting that we observed high velocity clouds in our Galaxy.

4. Discussion

A great majority (73%) of our galaxies are of type Im (26) and Ir (162), about 20% are of type Sph/Ir (12) and Sph (39), while the rest of 8% is a collection of different types from spiral to Im/Sm and BCD. The detection rate of our sample galaxies depends on the morphological type. 75% of the spirals (type S0 to Sm/Im and BCD) were detected; the detection rate for types Im and Ir is very similar close to 60%, whereas the detection rate for types Sph/Ir and Sph is considerable lower at 33 and 23%, respectively. The detection rate depends on the optical surface brightness (SB) class, too. From high SB to low, very low, and extremely low SB the detection rate decreases from 70% to 58%, 49%, and 43%, respectively. This trend reflects the type dependence and the fact that we deal with fainter galaxies as we descend from high SB to very low SB, the median absolute magnitudes for the detected galaxies change from −15.43 (H) to −13.92 (VL) for our brightness classes.

A number of the galaxies within the present sample are associated with nearby groups of galaxies (e.g. Tully 1988) according to their position, radial velocity and relative resolution:

NGC 672 group: kk 13, kk 14, kk 15;
NGC 784 group: kk 16, kk 17;
Maffei group: kk 19, kk 21, kk 22, kk 23, kk35 kk 44;
Orion group: kk 49;
M 81 group: kk 81, kk 83, kk 85, kk 89, kk 89, kk 91;
Leo group: kk 94;
CVn cloud: kk 109, UGC 7298, kk 137, kk 141, kk 144, kk 148, kk 149, kk 151, kk 154, kk 158, kk 160, kk 191, kk 206, kk 220, kk 230;
Centaurus group: kk 170, kk 179, kk 182, kk 190, kk 191, kk 195, kk 197, kk 200, kk 211, kk 217, kk 218;
NGC 6946 group: kk 250, kk 251, kk 252;

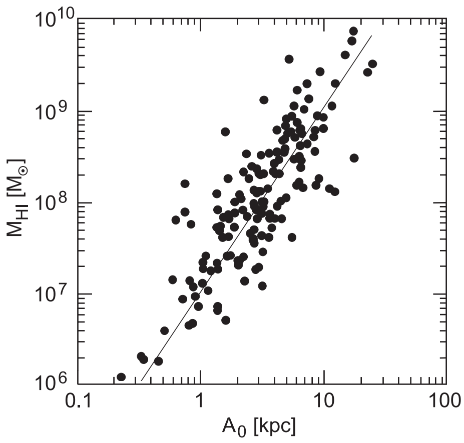

Fig. 6. The total mass of neutral hydrogen $M_{\rm HI}$ of the galaxies in our sample is plotted versus the linear extent (in kpc). The full line represents the regression line for the KKT sample (Huchtmeier & Richter 1988)

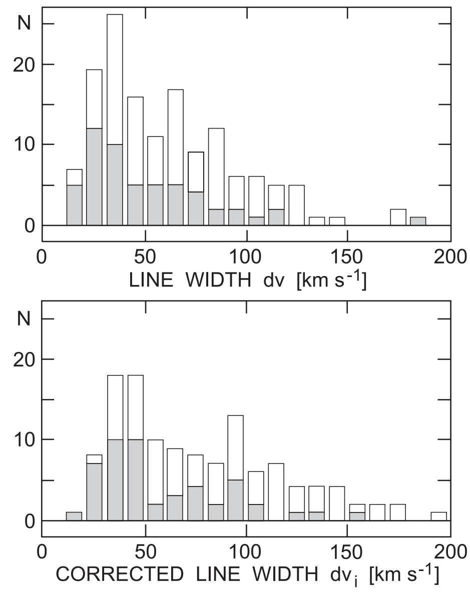

Fig. 7. The distribution of line widths of our galaxy sample is given for the observed values (dv) in the upper panel and for the (for inclination corrected values (dv_i) in the lower panel. Galaxies within the Local Volume (i.e. within 10 Mpc) are marked by the shaded areas

Virgo cluster: kk 111, kk 127, kk 128, kk 140, NGC 4523, IC3517, kk 164, kk 168, kk 169, kk 172, kk 173, U 8091.

There are a few cases of high $M_{\rm HI}/L_B$ values in Table 2. Four of the five galaxies with $M_{\rm HI}/L_B \geq 5$ are actually found to be confused by emission from nearby galaxies (see footnotes to Table 2).

The present sample of galaxies as presented in Tables 1 and 2 will be discussed now in some detail with the help of global parameters. The distribution of radial velocity (v_0, corrected for the rotation of our galaxy) is given in Fig. 4. Apart from a few background objects most of the galaxies belong to the local supercluster, about 25% are within the Local Volume. From this situation it is clear that the great majority of the galaxies in the present sample are dwarfish in nature. This will be shown more convincingly below when we compare several other global parameters of these objects.

Next we will look at the optical linear diameter A_0 (in kpc). The histogram in Fig. 5 presents the number of galaxies binned in intervals of 0.5 kpc width. The distribution of the optical linear diameters of our galaxies extends from 0.2 kpc to 26 kpc, yet the great majority is smaller than 8 kpc in diameter (in the de Vaucouleurs D_{25} system). Galaxies in the Local Volume (indicated by shaded areas) are even smaller with a median value of 1.4 $\pm$ 0.2 kpc.

Now we will use the correlation of two global parameters to compare the present sample of galaxies with the previously known galaxies in the Local Volume. In Fig. 6 the total mass of neutral hydrogen $M_{\rm HI}$ of the galaxies is plotted versus their linear extent A_0 for this sample of galaxies. The full line is the regression line for the KKT sample (Huchtmeier & Richter 1988). This regression line seems to be an excellent fit for the present sample, too. The average HI mass of the galaxies in the Local Volume is 4.6 10^7 $M_\odot$.

The HI masses in Fig. 6 cover a range from 10^6 to 10^{10} solar masses. The HI luminosity function for galaxies has been studied with galaxies of 10^7 and more solar masses in HI so far. With the data of the new dwarf galaxies within the Local Volume we will be able in the end to discuss the HI luminosity function starting from 10^6 solar masses.

The galaxies in our sample have small line widths on the average. In Fig. 7 we present the distribution of observed line widths in the upper panel and the (for inclination) corrected line widths in the lower panel. The optical axial ratio has been used here to derive the inclination. Galaxies within the Local Volume are indicated by the shaded areas. The peak of the line width distribution of the galaxies within the Local Volume is 39 km s^{-1} for the uncorrected and 47 km s^{-1} for the corrected line widths.

The three global parameters we have considered so far point altogether toward the dwarfish character of the Local Volume objects in our sample: the average linear diameter of 1.4 $\pm$ 0.2 kpc (Fig. 5), the mean total HI mass of 4.6 10^7 $M_\odot$ and the small line width of less than 50 km s^{-1}.

Two more global parameters are shown in Fig. 8, pseudo HI surface density $\Sigma_{\rm HI}$ and the relative HI content $M_{\rm HI}/M_{\rm T}$. The pseudo HI surface density is obtained by dividing the total HI mass $M_{\rm HI}$ of the galaxy by the disk area of the galaxy as defined by its optical diameter A_0. This quantity is given in units of solar mass per square

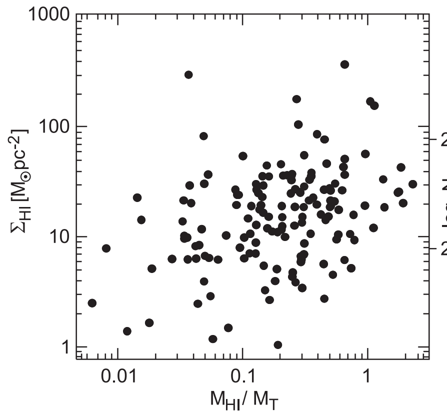

Fig. 8. The pseudo column density of neutral hydrogen (Σ_{HI} in $M_{\odot}\,\mathrm{pc}^{-2}$) of our sample as plotted versus the relative HI-content ($M_{\mathrm{HI}}/M_{\mathrm{T}}$)

parsec as well as in the usual HI column density N_{HI} in atoms cm^{-2}. This quantity is plotted versus the relative HI content $M_{\mathrm{HI}}/M_{\mathrm{T}}$. Our galaxies fill the usual range in HI surface density as well as in relative HI content as observed for normal galaxies (e.g. HR). The present sample of galaxies is relatively rich in HI. Some of the scatter in the diagram is due to uncertainties in observed quantities, especially the inclination which is used to correct the line width which itself enters the total mass calculation by the square. The optical diameters are uncertain for galaxies at low galactic latitudes due to the high foreground extinction, e.g. Cas 2, ESO 137–G27, BK12, ESO 558–11. If we exclude the confused galaxies and those with heavy galactic extinction all entries in Fig. 8 with $\Sigma_{\mathrm{HI}} \geq 100\ M_{\odot}\,\mathrm{pc}^{-2}$ are gone. Low values of the HI surface density are not only due to the uncertainties of observational data, the gas content of dwarf galaxies is very sensitive to outside influences (tidal interactions) due to their shallow gravitational potential.

Finally we plot the HI surface brightness versus the optical surface brightness (Fig. 9). The surface brightness class (Table 1, Col. 7) has been coded from 4 to 1 from high SB to extremely low SB in steps of 1. The different errors of the mean values of each class essentially depend on the different population size of each SB class. However, there is a definite trend of the HI surface density to grow with increasing optical SB by a factor of 2 to 4 (e.g. van der Hulst et al. 1993; de Blok 1997).

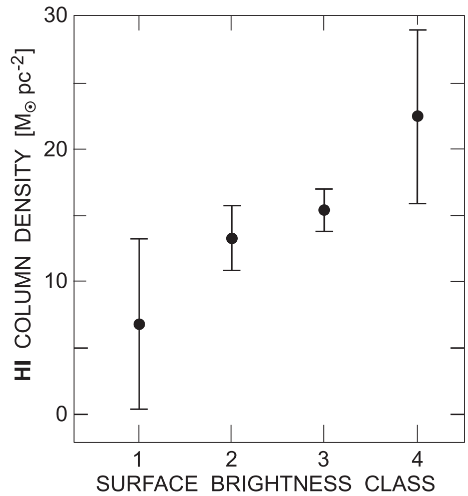

Fig. 9. This figure presents a correlation between the pseudo HI column density with the optical surface brightness of the galaxy in our actual sample. The surface brightness class is taken from KK98; 1 = extremely low, 2 = very low, 3 = low, 1 = high SB. The error bars correspond to twice the rms error of the mean of each SB class

5. Conclusion

In this paper we presented an HI search for 257 candidates for nearby dwarf galaxies. A detection rate of 60% on the average is quite high keeping in mind the limited velocity band and the fact that single-dish telescopes are literally "blind" for weak emission in the velocity range of the local HI emission (i.e. within -140 to $+20\ \mathrm{km\,s^{-1}}$) and for 20% of HI-poor (spheroidal and Sph/Ir) objects in the sample. Most of the detected galaxies are located within the local supercluster, and about 25% are members of the Local Volume. The dwarfs within the Local Volume have a mean linear diameter of 1.4 ± 0.2 kpc, a mean observed linewidths of 39 $\mathrm{km\,s^{-1}}$, and a mean total HI mass of 4.6 $10^{7}\ M_{\odot}$. The smallest galaxies have HI masses of just over 10^{6} solar masses. Once this full-sky survey will be finished we will be able to discuss the luminosity function of the Local Volume including these tiny dwarf galaxies. This investigation is especially needed as recent determinations of the galaxy luminosity function exhibit an increase for low mass objects. The exact value of this increase will be important for deriving the mass density in the local universe.

Acknowledgements. The Australia Telescope is funded by the Commonwealth of Australia for operation as a National Facility managed by CSIRO.

The Nançay Radio Astronomy Observatory is the Unité Scientifique de Nançay of the Observatoire de Paris, associated as Unité de Service et de Recherche (USR) No. B704 to the French Centre National de la Recherche Scientifique (CNRS). The Observatory also gratefully acknowledges the financial support of the Conseil Régional of the Région Centre in France.

This research has made use of the NASA/IPAC Extragalactic Database (NED) which is operated by the Jet Propulsion Laboratory, California Institute of Technology, under contract with the National Aeronautics and Space Administration.

This work has been partially supported by the Deutsche Forschungsgemeinschaft (DFG) under project No. 436 RUS 113/470/0 and Eh 154/1-1.

References

Burton W.B., Verheijen E.B., Kraan-Korteweg R.C., Henning P.A., 1996, A&A 293, L33
Cote S., Freeman K.C., Carignan C., Quinn P.J., 1997, AJ 114, 1313
de Blok W.J.G., 1997, Ph.D. Thesis, University of Groningen
Gallagher J.S., Littleton J.E., Mathews L.D., 1995, AJ 109, 2003
Hartmann D., Burton W.B., 1997, Atlas of Galactic Neutral Hydrogen. Cambridge University Press, Cambridge
Huchra J., 1995, A catalog of galaxy redshifts
Huchtmeier W.K., Bohnenstengel H.-D., 1981, A&A 100, 72
Huchtmeier W.K., Lercher G., Seeberger R., Saurer W., Weinberger R., 1995, A&A 293, L33
Huchtmeier W.K., van Driel W., 1996, A&A 305, L25
Huchtmeier W.K., Karachentsev I.D., Karachentseva V.E., 1997, A&A 322, 375
Huchtmeier W.K., Richter O.G., 1988, A&A 203, 237 (HR)
Huchtmeier W.K., Richter O.-G., 1989, A general catalog of HI observations of galaxies. Springer-Verlag, New York
van der Hulst J.M., Skillman E.D., Smith T.R., Bothun G.D., McGaugh S.S., de Blok W.J.G., 1993, AJ 106, 548
Karachentsev I.D., Makarov D.I., Huchtmeier W.K., 1999, A&AS (in press)
Karachentseva V.E., Karachentsev I.D., 1998, A&AS 127, 409
Karachentseva V.E., Karachentsev I.D., Richter G.M., 1999, A&AS 135, 221
Kraan-Korteweg R.C., Tammann G.A., 1979, Astron. Nachr. 300, 181 (KKT)
Kraan-Korteweg R.C., Loan A.J., Burton W.B., et al., 1994, Nat 372, 77
Matthews L.D., Gallagher J.S., Littleton J.E., 1995, AJ 110, 581
Paturel G., Fouque P., Bottinelli L., Gouguenheim L., 1992, Catalogue of Principal Galaxies, Lyon (PGC)
Roberts M.S., 1969, AJ 74, 859
Schombert J.M., Bothun G.D., Schneider S.E., McGaugh S.S., 1992, AJ 103, 1107
Tully R.B., 1988, Nearby Galaxy Catalog. Cambridge Univ. Press

Table 1. List of new Local Volume dwarf candidates

KK	R.A. (1950.0)	Dec.	a	b	Type	S.B.	B_t	Ref.(B)	A_b	Identification
	h m s	° ′ ″	arcmin							
1	2	3	4	5	6	7	8	9	10	11
1	00 12 31.6	−38 45 43	0.9	0.35	Im	H				AM 0012–384
2	00 12 53.5	−21 43 17	2.3	1.3	S0	H	13.12	NED	0.06	NGC 59
3	00 13 00.0	−32 27 36	1.5	1.3	Im	H				FG 11
4	00 29 27.4	−33 32 30	0.9	0.8	Sph/Ir	L				FG 16, AM 0029–333
5	00 32 52.7	+36 13 21	5:	3:	Sph	EL				And III
6	00 34 43.3	+47 53 57	0.5	0.48	Ir	L				
7	00 35 18.6	−43 46 46	0.6	0.4	Im	H				AM 0035–434
261	00 38 30.5	−26 32 28	0.6	0.3	Ir	VL				
8	00 42 56.2	+37 45 51	4:	3:	Sph	EL				And I
9	00 46 51.9	−18 20 48	1.2	1.1	Sph	L				K 2
10	00 47 56.0	−20 10 44	1.3	1.2	Sph/Ir	L				FG 24
12	01 13 41.9	+33 09 20	4:	2.5:	Sph	EL				And II
13	01 39 29.5	+26 06 57	0.7	0.35	Ir	L	16.57	UH	0.29	
14	01 41 54.0	+27 02 14	1.6	0.6	Ir	L	17.47	6m	0.24	
15	01 43 53.6	+26 33 07	0.6	0.18	Ir	VL	18.22	UH	0.26	
262	01 43 55.7	+14 26 33	1.0	0.7	Ir	H	15.3	IK	0.08	UGC 1242
263	01 47 10.5	+28 40 03	0.7	0.55	Ir	L	18.4	IK	0.18	
16	01 52 30.2	+27 42 34	0.8	0.28	Ir	L	16.3	IK	0.29	
17	01 57 18.1	+28 35 26	0.6	0.3	Ir	L	17.2	IK	0.20	
18	01 57 22.0	+67 30 36	1.3	0.9	Sph?	EL				
264	02 01 46.3	+72 30 23	0.8	0.8	Ir	L	18.7	IK	2.96	
19	02 02 02.4	+68 45 57	2.2	1.7	Ir	L	16.38	6m	4.44	Cas 1
20	02 31 39.9	+22 21 45	1.2	0.7	Sph	VL				
21	02 31 52.2	+59 09 42	2.4:	1.0:	Ir	EL	19.5	IK	4.19	MB 1
22	02 51 54.1	+58 39 35	1.6	0.5	Ir	EL	19.8	IK	5.68	MB 3
23	02 53 01.1	+58 42 37	2.0:	0.3:	SB	EL	18.8	IK	6.20	Cas 2
24	02 53 54.5	+17 15 25	0.6	0.4	Ir?	L				
25	03 07 59.9	+60 09 28	2.8	0.8	Ir?	VL	19.0	IK	6.00	
26	03 18 53.2	+62 36 27	1.8	0.9	Ir	L				Cam C
27	03 20 29.5	−66 30 04	1.2	0.4	Ir	L				
28	03 28 35.2	+47 37 28	1.4	0.8	Ir	H	15.04	NED	2.41	UGC 2773
265	03 29 09.1	+67 56 36	2.0	0.8	Ir	L	17.0	IK	3.45	K 37=BK 7
29	03 33 18.9	−61 15 37	1.8	0.9	Im	EL	16.38	NED	0.05	FG 82, AM 0333–611
266	03 33 44.4	+67 26 00	2.0	0.7	Ir?	L	17.0	IK	3.44	BK 8
30	03 37 12.6	+68 02 50	1.0	0.5	Sph?	VL	18.6	IK	2.34	
31	03 37 26.2	−18 49 42	0.7	0.6	Ir/Sph	L				
32	03 37 26.8	+19 35 30	0.8	0.7	Ir	L				
267	03 38 25.0	+68 06 11	2.2	0.3	Ir?	L	17.7	IK	2.24	BK 12
33	03 38 39.9	+67 52 57	0.4:	0.4:	Ir	VL				
34	03 38 56.9	−45 30 52	1.5	1.5	Im	H	14.84	NED	0.0	AM 0338–453
35	03 40 23.7	+67 42 26	2.5	1.7	Ir	VL	17.2		2.5	
36	03 42 47.0	+67 30 57	1.0	0.6	Ir	L	17.4	IK	2.67	
37	03 47 15.0	+70 56 34	0.9	0.4	Ir?	VL	16.9	IK	2.37	BK 17
268	03 53 22.5	+69 08 24	1.1	0.6	Sph?	L	17.2	IK	2.72	BK 19
38	03 58 47.0	−62 38 57	0.7	0.5	Im	H				AM 0358–623

Table 1. continued

KK	R.A. (1950.0)	Dec.	a	b	Type	S.B.	$B_{\rm t}$	Ref.(B)	A_b	Identification
	h m s	° ′ ″	arcmin							
1	2	3	4	5	6	7	8	9	10	11
269	03 59 34.8	+71 25 44	1.2	0.5	Ir	VL	17.0	IK	1.17	BK 21
39	04 00 06.0	+71 20 00	1.1:	0.9:	Ir?	EL	18.5	IK	1.12	
40	04 05 56.0	−55 27 21	1.6	1.0	Im	H	14.73	NED	0.0	AM 0405–552
270	04 06 44.0	+70 38 33	0.9	0.4	Ir	L	16.6	IK	1.17	
41	04 19 26.7	+72 41 27	3.7	2.1	Sph?	VL				Cam A
42	04 39 44.4	+61 15 47	0.6	0.6	Ir?	VL				
43	04 45 11.0	−36 00 18	2.2	0.8	Im/Sm	H	15.23	NED	0.0	AM 0445–360
271	04 46 40.8	+67 04 29	0.6	0.35	Sph?	L	17.7	IK	0.92	
44	04 48 03.3	+67 01 02	2.2	1.1	Ir	L	16.71	UH	0.93	
45	05 21 35.2	−34 37 13	0.55	0.4	Im	H	16.8	IK	0.0	AM 0521–343
46	05 23 05.4	−87 05 14	1.4	0.7	Im	L	15.90	NED	0.61	FG 154, AM 0522–870
47	05 27 49.0	−87 37 36	1.0	0.45	Im	L				AM 0528–873
48	05 28 26.3	−24 54 44	1.7:	0.3:	Im/Sm	VL	16.17	NED	0.06	AM 0528–245
49	05 39 00.7	+06 39 28	0.7	0.5	Im?	H	16.1	IK	2.85	
50	05 47 25.5	+02 52 10	0.5	0.4	Ir	VL	18.3	IK	2.87	
51	05 48 47.9	+02 53 48	2.1	0.5	Ir	EL				
52	06 02 18.4	−19 37 03	1.2	0.5	Ir	L	17.06	NED	0.38	
53	06 12 51.5	−51 31 41	1.1	0.6	Im	L	16.54	NED	0.15	AM 0612–513
54	06 24 16.7	−26 14 06	0.6	0.3	Ir	H	15.6	IK	0.43	AM 0624–261
55	06 37 55.8	−40 40 24	0.7	0.45	Ir	VL	16.23	NED	0.33	AM 0637–404
56	06 39 49.0	+36 41 03	1.3	0.4	Ir?	L	17.9	IK	0.66	
57	07 04 49.9	−21 57 29	1.9	1.1	Ir	L	15.8	IK	2.81	
58	07 07 56.2	−51 23 08	1.4	1.1	Ir	L	15.31	NED	0.25	FG 203
59	07 17 41.2	−57 19 06	2.1	1.6	Im/Sm	VL	16.1	IK	0.43	FG 206, AM 0717–571
60	07 20 23.0	+46 06 10	1.1	0.4	Ir	L				
61	07 29 13.1	+66 59 40	3:	2:	Sph	VL				DDO 44
62	07 31 50.6	+42 12 13	0.6	0.4	Ir	L	17.6	IK	0.21	
64	07 39 30.0	+69 41 09	0.6	0.2	Ir	L	16.6	IK	0.12	
65	07 39 40.2	+16 40 47	0.9	0.5	Ir	H	15.6	NED	0.09	
66	07 44 05.4	+40 18 42	0.7	0.4	Ir	L	17.0	IK	0.22	
67	08 00 34.9	+15 17 03	1.0	0.5	Ir	L				
68	08 27 17.0	−84 58 57	1.1	1.0	Ir?	H				
69	08 49 44.1	+33 59 13	2.4:	1.8:	Sph?	EL	16.8	IK	0.07	
70	08 52 16.3	+33 45 02	1.1	1.0	Sph?	EL				
71	09 06 56.7	−23 09 51	0.45	0.35	Ir/Sph	L	18.7	IK	0.73	AM 0906–231
72	09 09 28.5	−23 46 35	0.6	0.5	Sph	L				
73	09 10 15.6	−24 02 05	0.9	0.8	Sph	L				
74	09 12 18.0	−23 20 55	0.8	0.4	Im	L				FG 247, AM 0912–232
75	09 12 48.9	−25 40 30	0.9	0.6	Ir	L	18.0	IK	0.73	
U5005	09 21 37.4	+22 29 20	1.3	0.9	S?	H	15.9	IK	0.10	UGC 5005
76	09 38 23.6	−76 21 41	2.1	0.8	Ir	L				
77	09 46 08.5	+67 44 25	2.4	1.8	Sph	VL				
78	09 47 23.6	+31 41 26	0.5	0.3	Ir	H	17.6	IK	0.03	
79	09 50 03.5	+29 32 46	0.6	0.4	BCD?	H	17.0	IK	0.02	
80	09 50 45.0	+29 40 57	1.1	0.6	Ir	L				

Table 1. continued

KK	R.A. (1950.0)	Dec.	a	b	Type	S.B.	B_t	Ref.(B)	A_b	Identification
	h m s	° ′ ″	arcmin							
1	2	3	4	5	6	7	8	9	10	11
81	09 53 00.8	+68 49 47	2.6	2.6	Sph	VL				K 61
82	10 00 25.3	−05 57 55	0.6	0.5	Ir	L	17.73	NED	0.05	
82	10 00 25.3	−05 57 55	0.6	0.5	Ir	L	17.73	NED	0.05	
83	10 01 18.0	+66 48 00	1.7	1.7	Sph	VL				DDO 71, K 63
84	10 03 05.8	−07 30 20	1.9	1.3	Sph	L				K 65
85	10 03 09.0	+68 04 19	2.0	1.0	Sph	L				K 64, UGC 5442
86	10 05 22.0	+30 44 09	1.0	0.6	Ir?	L				MCG 5–24–18
87	10 12 37.6	−44 36 08	1.2	1.0	Sm?	H				AM 1012–443
88	10 13 57.4	−39 44 23	0.9	0.5	Ir	VL				AM 1013–394
89	10 22 47.6	+67 54 32	2.0	2.0	Sph	VL	15.8	NED	0.06	DDO 78
90	10 26 26.1	+23 01 57	1.0	0.15	Ir/S	VL	16.8	IK	0.0	
91	10 31 00.0	+66 16 00	1.0	0.8	Sph	VL				BK 6N
92	10 33 30.1	+27 47 52	0.8	0.7	Ir	L	16.9	IK	0.04	
93	10 43 45.8	+14 17 16	1.2	1.1	Ir	VL				
94	10 44 18.1	+13 15 48	1.2	0.6	Ir	VL	17.9	IK	0.04	
95	10 46 03.6	+64 59 20	2.2:	1.7:	Ir	VL				UGCA 220
96	10 47 48.8	+12 37 34	1.2:	0.8:	Sph	EL				
97	10 55 35.3	+20 22 35	0.7	0.5	Ir	L				
98	11 09 37.7	+17 01 32	0.9	0.4	Sph/Ir	VL	17.4	IK	0.0	F 640-3
99	11 11 11.2	−47 46 02	0.35	0.25	Im	H				AM 1111–474
100	11 11 22.9	+11 36 10	1.2	0.5	Ir	VL				
101	11 14 19.1	−32 22 39	0.7	0.4	Sph?	L				AM 1114–322
102	11 20 21.2	+19 44 58	0.6	0.4	Ir?	L	17.1	IK	0.0	F 570–3
103	11 21 03.8	+19 31 52	0.6	0.4	Sph	VL				
104	11 26 14.5	+18 33 25	1.1	0.7	Ir?	VL	17.1	IK	0.0	F 571–10
105	11 26 40.7	+46 23 23	0.8	0.5	Ir?	L	16.6	IK	0.0	
106	11 27 08.7	+52 40 54	0.8	0.7	Sph?	VL	16.7	IK	0.0	K 78
107	11 31 40.1	+17 26 14	0.7	0.4	Ir	L				
108	11 37 23.0	+46 45 29	0.7	0.6	Sph?	VL	17.7	IK	0.01	
109	11 44 33.5	+43 56 59	0.6	0.4	Ir?	L	17.5	IK	0.0	
110	11 46 01.0	+56 11 44	0.6	0.6	Ir?	L				
111	11 51 27.3	+16 59 55	0.6	0.45	Ir?	L	17.0	IK	0.14	
113	11 52 17.9	+47 04 59	0.5	0.3	Ir?	VL				
114	11 53 55.1	−36 27 39	0.5	0.35	Im	H				
115	11 55 37.1	+49 09 34	0.7	0.55	Im	H	16.2	IK	0.05	MCG 8–22–48
116	11 56 18.5	+46 00 45	1.3	0.7	Ir	L	15.8	IK	0.0	UGCA 259
117	11 57 24.6	+44 59 50	0.6	0.6	Ir?	L	17.1	IK	0.0	
118	11 58 42.9	+54 03 01	0.6	0.15	Ir	VL				
119	11 59 13.5	+28 38 26	0.8	0.7	Ir	L	17.0	IK	0.0	
120	12 00 56.2	−25 11 35	2.5	1.9	Im/Sm	L	16.8	IK	0.43	FG 320;AM 1200–251
121	12 02 52.3	+43 59 13	1.1	0.6	Ir	VL				
122	12 04 04.8	+55 02 38	1.0	0.25	Ir	L	16.4	IK	0.0	
123	12 04 20.5	+17 37 01	0.9	0.2	Ir	L				
124	12 06 16.1	+52 50 29	0.5	0.3	Ir?	EL				
125	12 10 16.9	+69 12 20	0.7	0.6	Sph?	VL				
126	12 10 47.5	+28 41 44	0.6	0.3	Ir	L	16.7	IK	0.02	

Table 1. continued

KK	R.A. (1950.0)	Dec.	a	b	Type	S.B.	B_t	Ref.(B)	A_b	Identification
	h m s	° ′ ″	arcmin							
1	2	3	4	5	6	7	8	9	10	11
127	12 10 51.5	+30 12 00	0.9	0.25	Ir	H	16.22	UH	0.04	
128	12 11 17.1	+05 37 54	0.6	0.4	Ir	L	17.0	IK	0.0	GR 5
129	12 11 38.9	+16 14 35	1.1	1.1	Sph	VL				K 88,VCC 108
U7298	12 14 02.2	+52 30 29	1.1	0.6	Ir	L	15.95	6m	0.04	UGC 7298
130	12 15 17.6	+28 45 09	0.6	0.3	Ir	L				K 95
131	12 15 58.1	+28 55 31	0.6	0.5	Sph/Ir	VL				K 98
132	12 16 38.5	+48 00 25	0.6	0.5	Sph/Ir	VL				
133	12 17 04.1	+43 39 50	0.4	0.3	Ir	L				
134	12 17 05.3	+47 43 54	0.3	0.3	Sph?	L				
135	12 17 09.5	+58 19 18	0.8	0.4	Ir	VL				
136	12 18 13.5	+47 16 43	0.5	0.5	Sph?	L				
137	12 19 13.0	+38 15 06	0.9	0.5	Ir	VL	16.08	UH	0.0	K 105
138	12 19 27.0	+28 31 09	0.9	0.5	Sph/Ir	VL	17.8	IK	0.08	
139	12 19 37.9	+40 01 23	0.9	0.4	Ir	L	16.7	IK	0.0	
140	12 20 15.7	+08 11 27	0.6	0.5	Ir	L	15.8	NED	0.0	VCC 584
141	12 20 23.2	+34 06 23	0.4	0.3	Ir	L	17.5	IK	0.0	
142	12 21 48.5	−42 00 57	1.0	0.5	Ir?	L				AM 1221–420
143	12 22 34.0	+61 20 20	1.0	0.7	Ir	L	16.59	UH	0.0	MCG 10–18–44
144	12 22 58.6	+28 45 33	1.5	0.5	Ir	L	16.5	IK	0.09	
145	12 24 18.6	+62 39 23	1.1	0.7	Ir	L	16.61	UH	0.01	UGC 7544
146	12 24 19.1	+13 27 15	1.0	0.35	Sm	L				DDO 124
147	12 25 20.3	−37 03 12	2.0	0.25	Im/Sm?	H	15.59	NED	0.20	AM 1225–370
148	12 25 32.4	+22 51 57	0.8	0.4	Ir	H	16.2	IK	0.07	UGC 7584
149	12 26 25.8	+42 27 20	0.8	0.45	Ir	L	15.01	NED	0.0	MCG 7–26–11
150	12 27 28.2	+08 12 24	1.1	0.7	Im	L				UGC 7636
151	12 27 57.5	+43 10 38	1.2	0.5	Ir?	L	15.8	IK	0.0	MCG 7–26–12
VPC873	12 30 02.9	+14 51 23	0.2	0.2	Ir	H				
152	12 30 58.4	+33 37 42	1.2	0.4	Ir	H	16.5	IK	0.03	MCG 06–28–9
N4523	12 31 16.9	+15 26 39	2.3	2.0	SBd?	H	14.42	NED	0.0	NGC 4523
I3517	12 31 58.8	+09 25 52	1.0	0.6	Ir	H	15.38	NED	0.0	IC3517
I3521	12 32 07.1	+07 26 12	1.2	0.6	BCD	H	13.98	NED	0.0	IC3521
153	12 32 44.4	+58 39 45	0.5	0.3	Ir	L				K 162
154	12 34 56.4	+39 01 12	0.7	0.4	Ir	H	15.74	6m	0.0	Arp 211
155	12 35 13.0	+07 22 42	1.2	1.0	Ir	L				UGC 7795
156	12 38 09.0	+47 38 21	0.5	0.2	Ir	L				
157	12 38 31.3	−40 53 03	1.7	0.4	Ir	VL				AM 1238–405
158	12 39 06.9	+40 05 13	1.1	0.7	Ir	L	16.7	IK	0.0	
159	12 40 48.0	+35 41 16	0.7	0.5	Ir?	L	17.4	IK	0.0	
160	12 41 35.8	+43 56 15	0.8	0.6	Ir	L	17.0	IK	0.0	
161	12 42 10.0	+71 03 52	1.1	0.7	Ir?	L	16.6	IK	0.0	K 195
162	12 42 57.3	+18 34 25	0.9	0.7	Ir?	EL				
163	12 43 37.6	+62 14 21	0.9	0.4	Ir?	VL				
164	12 45 26.9	+04 42 24	1.1	0.6	Ir	H	15.5	IK	0.01	
165	12 46 27.6	+32 14 33	0.7	0.7	Ir?	L				
166	12 46 49.5	+35 53 05	1.7	1.0	Sph	L				

Table 1. continued

KK	R.A. (1950.0)	Dec.	a	b	Type	S.B.	B_t	Ref.(B)	A_b	Identification
	h m s	° ′ ″	arcmin							
1	2	3	4	5	6	7	8	9	10	11
167	12 49 17.8	+26 22 56	0.8	0.5	Ir?	L	16.7	IK	0.02	
168	12 50 37.8	+03 42 44	0.5	0.4	Ir?	VL	17.3	IK	0.0	
169	12 50 41.3	+12 54 24	0.8	0.6	Ir	L	17.1	IK	0.05	
170	12 52 11.5	−28 04 12	0.8	0.6	Im	L	17.01	NED	0.30	AM 1252–280
171	12 53 03.1	+33 15 22	0.7	0.6	Ir?	L				
172	12 54 14.0	+12 12 10	1.3	1.0	Ir	L	16.3	IK	0.07	UGC 8061
173	12 56 07.5	+18 04 58	0.7	0.45	Ir	L	17.2		0.11	
U8091	12 56 10.5	+14 29 17	1.6	0.9	Ir	H	14.68	NED	0.04	UGC 8091
174	12 56 29.7	−49 21 08	2.2	1.6	Ir	L	16.52	NED	0.89	FG 363
175	12 56 38.7	+35 45 03	0.6	0.4	Ir?	L	17.1	IK	0.01	
176	12 57 17.1	−19 08 26	1.7	0.7	Sph/Ir	VL	17.5	IK	0.17	
177	13 00 15.2	+22 16 02	0.8	0.7	Sph?	VL				F 575-1
178	13 00 32.8	+26 20 46	0.8	0.3	Ir	L				F 508-1
180	13 02 02.1	+18 01 37	1.4	0.7	Sph/Ir	VL				F 575-4
181	13 02 09.2	+27 02 31	0.7	0.6	Ir	L	17.25	NED	0.0	F 508-v1
182	13 02 12.8	−39 48 54	1.0	0.55	Ir	L	16.33	NED	0.37	
272	13 03 33.1	−49 33 38	1.6	0.6	Ir	L				ESO 219-G027
183	13 04 14.8	+18 16 08	0.6	0.45	Sph?	L	17.9		0.07	
185	13 06 36.8	+33 28 07	0.6	0.5	Ir	L				
186	13 07 03.5	−23 16 35	0.7	0.3	Im	H				AM 1307–231
187	13 07 23.3	−26 19 43	1.0	0.8	Im	H	17.3	IK	0.31	AM 1307–263
188	13 08 47.7	+37 26 39	0.9	0.6	Ir	L				
191	13 11 24.8	+42 18 31	0.8	0.7	Sph?	EL	18.2	IK	0.0	
192	13 12 02.7	+36 50 08	0.7	0.5	Sph?	L	16.7	IK	0.0	
193	13 13 16.4	+41 45 55	0.6:	0.6:	Ir/Sph	EL				
194	13 15 07.3	+44 39 44	0.6:	0.4:	Ir?	VL				
195	13 18 20.5	−31 16 05	1.3	0.6	Ir	VL	17.4	IK	0.23	
196	13 18 49.9	−44 48 05	0.6	0.4	Ir?	L				AM 1318–444
198	13 20 07.0	−33 18 23	0.6	0.5	Sph?	L				
199	13 20 31.4	−28 56 34	0.4	0.35	Ir	EL				
200	13 21 48.1	−30 42 43	1.3	0.8	Im	H	16.67	NED	0.19	K 15, AM 1321–304
201	13 22 20.0	−37 21 50	1.3	0.7	Ir/Sph	VL				AM 1321–372
202	13 22 37.7	−29 00 39	0.6	0.45	Ir	L				
204	13 25 28.7	−37 54 37	1.6	1.1	Ir?	L	14.97	NED	0.24	FG 393, AM 1325–375
205	13 26 46.8	+67 53 28	1.2	0.5	Ir	L				UGC 8509
206	13 31 18.6	+49 21 30	1.0	0.6	Ir	H	14.6	PGC		MCG 8–25–18
207	13 31 31.6	+56 45 26	0.6	0.4	Ir?	VL				
208	13 33 46.5	−29 19 00	6::	2.5:	Ir	EL	14.3			
209	13 35 52.8	+49 22 26	0.4	0.25	Ir	L				
210	13 37 31.2	−31 26 47	1.4	0.6	Im?	L	16.57	NED	0.11	FG 403
212	13 39 12.6	+43 32 31	0.8	0.6	Ir?	L	15.9	IK	0.0	MCG 07–28–51
215	13 40 45.2	−45 39 22	0.5	0.5	Im	L				AM 1340–453
216	13 41 24.2	+43 42 43	1.1	0.5	Ir	H	14.8	NED	0.0	UGC 8688
218	13 43 48.7	−29 43 47	1.7	0.7	Sph?	VL				
219	13 45 21.9	+39 37 26	0.7	0.4	Ir?	L	17.3			

Table 1. continued

KK	R.A. (1950.0)	Dec.	a	b	Type	S.B.	B_t	Ref.(B)	A_b	Identification
	h m s	° ′ ″	arcmin							
1	2	3	4	5	6	7	8	9	10	11
220	13 45 22.2	+33 27 25	0.8:	0.7:	Ir	L	16.5	IK	0.0	
223	13 46 07.8	+40 48 08	0.4	0.3	Ir?	L	17.4	IK	0.0	
224	13 46 52.8	+43 50 54	1.0	0.4	Ir	L	16.9	IK	0.0	
225	13 52 51.5	+37 55 42	0.45	0.3	Ir	L				
226	13 53 01.2	−45 24 47	1.1	0.7	Ir	L				
227	13 54 03.7	+40 32 50	0.7	0.45	Ir	L				
228	13 57 21.1	+52 36 16	0.9	0.8	Ir?	L	16.6	IK	0.0	UGC 8914
229	13 59 54.3	−46 51 45	0.8	0.6	Ir	L	16.55	NED	0.49	AM 1359–465
230	14 05 01.5	+35 18 09	0.6	0.5	Ir	VL	16.9	IK	0.0	
274	14 06 37.4	−30 02 30	0.8	0.6	Im	H	16.8	IK	0.22	
231	14 15 34.6	+23 18 21	0.8	0.3	Ir	L				
275	14 16 00.0	−45 05 15	1.2	0.6	Im	H	14.62	NED	0.30	AM 1415–450
232	14 40 48.0	+50 01 40	0.9	0.5	Ir	VL	17.2	IK	0.05	
233	14 45 51.4	+53 02 31	1.1	0.7	Ir	L	15.9	IK	0.0	MCG 9–24–40
234	14 57 13.6	−51 31 55	1.7	0.6	Ir	VL				FG 434
236	15 04 09.5	+56 03 24	0.9	0.7	Sph?	VL	19.17	UH	0.01	
237	15 06 46.1	+56 27 03	0.7	0.5	Ir?	L	18.21	UH	0.17	K 233
238	15 11 59.0	−22 56 23	0.8	0.6	Im	L	17.11	NED	0.47	FG 458, AM 1511–225
239	15 25 33.2	−42 36 36	1.9	0.7	Ir	L				FG 444
240	16 22 23.0	−59 50 33	2.9	0.7	Sm?	L	14.8	IK	0.90	ESO 137- G27
241	16 22 59.4	−60 20 53	1.6	1.0	Ir	VL	16.6	IK	0.89	FG 447
242	17 53 18.0	+70 08 41	0.8	0.6	Sph?	EL	19.0	IK	0.14	
243	18 18 05.0	−62 17 44	0.9	0.6	Ir	L	16.59	NED	0.44	FG 458, AM 1818–622
245	19 16 17.0	+63 52 54	1.5	1.2	BCD	H				NGC 6789
246	20 00 48.0	−31 49 24	1.2:	0.5:	Ir	VL	17.06	NED	0.44	FG 492
247	20 04 51.7	−61 12 30	0.9	0.6	Ir	L				AM 2004–611
249	20 25 58.8	−31 51 07	0.8	0.4	Ir	L	15.65	NED	0.26	AM 2025–315
250	20 29 14.4	+60 16 22	1.8	0.8	Ir	VL	15.74	UH	1.31	UGC 11583
251	20 29 31.9	+60 11 03	1.6	0.8	Ir?	VL	16.49	UH	1.28	
252	20 30 33.5	+60 38 34	0.9	0.9	Sph?	VL	16.15	6m	1.95	
253	20 33 30.7	−69 21 58	1.0	0.9	Ir	L				AM 2033–692
254	20 33 46.2	+60 55 12	1.5	0.9	Ir?	EL				
255	21 54 21.4	−60 32 42	2.5	1.2	Ir	L	16.39	NED	0.0	FG 532, AM 2154–603
256	22 09 04.6	−43 25 29	0.6	0.5	Im	L				AM 2209–432
257	22 19 25.2	−48 39 26	2.2	1.3	Ir	L	15.3	IK	0.0	FG 545
258	22 37 56.3	−31 03 40	1.6	0.8	Ir?	L				K 20, FG 554, AM 2237–310
259	23 09 36.4	−44 03 01	4:	2.2:	Sm?	L				FG 569
260	23 11 46.9	−43 52 39	4.5	1.8	Ir	VL				

Table 2. List of new Local Volume dwarf candidates

KK No.	HI-flux Jy km s^{-1}	$S_{\max}$ mJy	velocity km s^{-1}	line width km s^{-1}	distance Mpc	M_{Bt}	HI mass $10^7 M_\odot$	M_{HI}/L_B	Comments
1	2	3	4	5	6	7	8	9	10
1		± 15							ATCA
2	2.66	57 ± 5.9	361 ± 2	50 62 76	5.4	−15.70	1.9	0.06	
3		± 24							N
4		± 35							N
5		± 3.5							
6		± 4							
7		± 20							ATCA
261	2.6	87 ± 13	2694 ± 2	32 40 41	35.9				
8		± 3.3							
9		± 8							
10		± 8.3							
12		± 3.6							
13	1.33	40 ± 7	357 ± 9	31 45 52	7.0	−13.15	1.5	0.53	
14	3.04	74 ± 6	420 ± 4	36 56 60	7.9	−12.53	4.4	2.73	
15	0.9	27 ± 6	368 ± 4	25 37 40	7.2	−11.69	1.1	1.51	
262	1.1	18 ± 7	7356 ± 3	105 124 126	99.8	−20.55	2.6	0.10	
263	0.92	25 ± 7	3841 ± 4	38 48 50	53.5	−15.49	6.1	2.48	
16	0.97	37 ± 5	206 ± 3	22 32 34	4.9	−12.76	5.6	0.28	
17	0.95	28 ± 5	156 ± 3	34 52 53	4.2	−11.34	5.1	0.95	
18		± 3.8							
264	3.28	34 ± 6	2918 ± 7	128 143 155	42.0	−17.38	130	0.98	
19	46.4	930 ± 4.6	35 ± 2	49	3.5	−15.87	14	0.39	
20	11.18	760 ± 2.2	−70.2 ± 1	14 20 22					
21	9.0	160 ± 10	189 ± 3	60 79 85	5.3	−13.57	6.0	1.44	
22	30.8	330 ± 30	96 ± 2	100 116 ..	3.9	−14.19			
23	205	960 ± 10	112 ± 2	187 202 204	4.1	−16.04	40.6	2.05	
24		± 3.7							
25	8.84	54 ± 3.7	2767 ± 2	260 273 277	39.5	−19.35	330	0.38	
26		± 2.6							
27		± 6							ATCA
28	26.1	349 ± 30	216 ± 1	81 92 96	4.3	−15.83	11.0	0.34	
265	26.1	202 ± 5	1378 ± 2	144 178 187	21.1	−18.33	280	0.83	
29	0.95	33 ± 3	1152 ± 5	38 52 56	12.6	−14.38	3.6	0.41	ATCA
266	54.24	629 ± 5.4	1434 ± 1	53 119 125	21.8	−18.60	600	1.41	
30	0.89	20 ± 2.3	1159 ± 6	45 59 61	18.1	−15.23	7.0	0.36	
31		± 8.1							
32		± 8							
267	2.14	32 ± 3.1	1140 ± 8	99 110 ..	20.4	−16.67	15.0	0.19	
33		± 5							
34	3.26	61 ± 4	1554 ± 3	60 77 80	18.4	−16.48	26.0	0.43	ATCA
35	0.82	35 ± 6	119 ± 3	25	2.1	−12.11	0.085	0.08	
36	3.45	33 ± 2.8	1267 ± 7	120 134 142	19.5	−16.87	31.0	0.35	
37	1.24	19.5 ± 2.9	836 ± 5	101 109 111	13.8	−16.41	5.4	0.09	
268	7.68	80 ± 2.2	1302 ± 2	120 134 138	20.0	−17.20	71	0.61	
38		± 7			7.3				ATCA

kk 4: heliocentric velocity = 1651 km s^{-1} (NED)
kk 7, 9, 10: undetected in HI (2)
kk 8, 12, 5: ANDI, II, III have been searched for HI within the radial velocity range −550 to 770 km s^{-1}
kk 18, 26, 32: undetected in HI (3)
kk 20: probably local HI
kk 35: resolved, companion to IC 342

Table 2. continued

KK No.	HI-flux Jy km s^{-1}	$S_{\rm max}$ mJy	velocity km s^{-1}	line width km s^{-1}	distance Mpc	$M_{B{\rm t}}$	HI mass $10^7 M_\odot$	$M_{\rm HI}/L_{\rm B}$	Comment
1	2	3	4	5	6	7	8	9	10
269	6.83	69 ± 5	1734 ± 2	120 133 136	25.8	−16.48	110	1.75	
39	2.0	21 ± 3.5	1732 ± 4	123 125 126	25.7	−14.73	17	1.42	
40	2.87	53 ± 5	1066 ± 2	101 109 112	11.4	−15.69	8.8	0.30	ATCA
270	4.6	110 ± 5	1159 ± 1	42 57 59	18.1	−16.09	36	0.85	
41		± 4.1							
42		± 5							
43	7.95	135 ± 26	1372 ± 6	46 111 130	15.7	−16.04	46	1.14	
271	0.79	12 ± 4	1581 ± 25		23.4	−15.22	10	0.54	
44	4.47	220 ± 15	77 ± 1	18 28 32	2.2	−11.14	0.50	1.12	
45	4.5	108 ± 15	955 ± 3	58 78 83	9.9	−13.26	10	3.29	
46	1.34	54 ± 5	1745 ± 3	43 48 50	21.0	−16.69	14	0.19	ATCA
47		± 6.4							ATCA
48	6.87	72 ± 4.9	1850 ± 2	96 120 121	22	−16.11	80	1.86	
49	8.92	140 ± 6.7	455 ± 2	55 84 87	4.8	−15.26	4.9	0.25	
50	2.08	21 ± 5.1	1776 ± 4	111 117 118	22.1	−16.36	23	0.42	
51		± 4.9							
52	5.85	74 ± 4.1	883 ± 2	94 105 108	9.1	−13.36	11	3.27	
53	0.85	29 ± 3	1253 ± 3	34 42 44	13.2	−14.39	3.5	0.39	ATCA
54	3.12	97 ± 6.4	491 ± 2	29 35 39	3.4	−12.71	0.89	0.47	
55	1.26	53 ± 5	824 ± 6	51 63 66	7.5	−13.59	1.7	0.39	ATCA
56	0.8	13 ± 3	2287 ± 6	58 83 85	30.6	−15.53	18.0	0.70	
57	7.26	73 ± 6	738 ± 3	116 132 136	6.7	−16.29	7.8	0.15	
58	2.15	82 ± 5	1054 ± 2	27 35 37	10.3	−15.07	5.4	0.32	ATCA
59	4.04	94 ± 6	1145 ± 2	21 45 67	11.5	−14.71	13.0	1.06	ATCA
60		± 4.3							
61		± 6							
62	2.71	37 ± 3.4	3100 ± 10	94 114 124	41.5	−15.90	110	3.07	
64	2.90	25 ± 3.5	3867 ± 5	125 153 156	53.5	−17.48	200	1.28	
65	3.43	86 ± 5	279 ± 5	38 60 68	2.2	−11.39	0.39	0.70	
66	1.61	17 ± 4	2976 ± 9	63 73 76	39.7	−16.38	60	1.08	
67		± 4.7							
68		± 6							ATCA
69	3.58	154 ± 6	464 ± 1	20 30 33	5.7	−12.12	2.6	2.42	
70		± 5							
71	1.54	49 ± 5.7	179 ± 3	27 38 41					
72		± 6							
73		± 5.3							
74		± 5.2							
75	1.40	27 ± 5.1	2866 ± 4	68 79 81	34.6	−15.54	40	1.56	
U5005	6.93	0.66 ± 3.6	3824 ± 4	109 122 126	49.7	−17.79	390	1.92	
76		± 7							ATCA
77		± 5.5							
78	15.8	204 ± 4.9	520 ± 2	80 99 104	6.3	−11.56	15	22.92	
79	1.2	20 ± 4	1638 ± 8	61 73 90	21.0	−14.75	13	1.01	
80		± 3.3							

kk 42: undetected in HI (3)
kk 61: undetected in HI (6), companion of NGC 2403
kk 65: companion of UGC 3974
kk 68: $v = 738$ km s^{-1} (1)
kk 69, 70: companion of NGC 2683
kk 71: local HI?
kk 74: undetected in HI (5)
kk 78: UGC 5272B, confusion with UGC 5272 at 1.9′

Table 2. continued

KK No.	HI-flux Jy km s^{-1}	S_{max} mJy	velocity km s^{-1}	line width km s^{-1}	distance Mpc	M_{Bt}	HI mass $10^8 M_{\odot}$	M_{HI}/L_B $10^9 M_{\odot}$	Comment
1	2	3	4	5	6	7	8	9	10
81		± 8.5							
82	3.94	165 ± 6	185 ± 1	21 31 35					
82	1.54	40 ± 3.2	3769 ± 6	35 48 55	47.3	−15.75	84	2.53	
83		± 6.2							
84		± 7							
85		± 5.7							
86		± 4.6							
87		± 6							ATCA
88		± 7							ATCA
89	0.84	27 ± 6.3	2788 ± 2	32 62 63	37.2	−17.11	27	0.25	
90	2.5	33 ± 3.8	1206 ± 4	95 105 108	14.9	−14.66	13	1.15	
91		± 6.8							
92	2.74	46 ± 3.9	1371 ± 3	71 79 81	17.5	−14.39	19.0	2.19	
93		± 6							
94	1.52	42 ± 3.5	833 ± 3	28 52 55	9.4	−12.21	3.1	2.63	
95		± 4.5							
96		± 6.7							
97		± 6.5							
98	0.78	9 ± 2.2	1205 ± 20	48 118 120	14.7	−13.68	4.0	0.87	
99		± 6							ATCA
100		± 6							
101		± 26							N
102	1.58	19.6 ± 3.3	3366 ± 5	86 117 120	43.8	−16.22	71	1.49	
103		± 8.8							
104	1.36	21 ± 5.6	1303 ± 3	62 114 116	16.2	−14.08	8.4	1.26	
105	2.04	28 ± 3.7	1555 ± 3	80 96 98	21.4	−15.18	21	1.16	
106	0.28	15 ± 4.2	592 ± 5	23 30 32	8.9	−13.09	0.53	0.20	
107		± 5							
108	6.99	72 ± 3.8	736 ± 3	88 110 138	10.5	−12.46	18	12.12	
109	0.7	37 ± 4.5	214 ± 3	11 23 36	3.4	−10.28	0.19	0.95	
110		± 4							
111	1.79	34 ± 3.8	980 ± 4	41 52 54	12.0	−13.62	0.61	1.40	
113		± 4.3							
114		± 31							N
115	2.29	37 ± 3	826 ± 4	74 91 94	12.0	−14.32	7.4	0.90	
116	5.81	129 ± 3.1	1151 ± 2	41 52 54	16.1	−15.41	35	1.53	
117	0.44	14 ± 3	1171 ± 10	38 50 54	16.3	−13.96	2.5	0.42	
118		± 4.8							
119	0.71	23 ± 3	841 ± 3	34 42 44	10.9	−13.23	2.0	0.65	
120	17.12	253 ± 6.5	1785 ± 1	70 85 89	20.8	−15.30	180	8.73	
121		± 3.4							
122	2.32	33 ± 4	850 ± 2	72 91 93	12.7	−14.52	8.5	0.85	
123		± 7.6							
124		± 4.6							
125		± 4							
126	1.24	25 ± 3.5	1028 ± 10	36 57 62	13.5	−14.17	5.1	0.71	

kk 82: 15′ from PGC 29086 ($v = 662$ km s^{-1})
kk 84: companion of NGC 3115
kk 87: heliocentric velocity 969 km s^{-1} (NED)
kk 88: heliocentric velocity 263 and 2982 km s^{-1} (6)
kk 89: highly probably member of M 81 group, HI emission probably not from this object
kk 94, 96: near Leo triplet
kk 103: heliocentric velocity 1894 km s^{-1} (NED)
kk 108: NGC 3782 ($v = 739$ km s^{-1}) at 7.6′ NW, definitely confused in HI

Table 2. continued

KK	HI-flux	$S_{\max}$	velocity	line width	distance	M_{Bt}	HI mass	$M_{\rm HI}/L_{\rm B}$	Comments
No.	Jy km s^{-1}	mJy	km s^{-1}	km s^{-1}	Mpc		$10^7 M_\odot$		
1	2	3	4	5	6	7	8	9	10
127	2.87	41 ± 4.4	131 ± 6	64 112 117	1.6	−10.23	0.18	0.92	
128	1.80	24 ± 3.2	1690 ± 2	56 73 76	21.0	−14.72	19	1.58	
129		± 6.1							
U7298	5.44	193 ± 6.5	172 ± 1	26 38 41	3.5	−12.01	1.6	1.66	
130		± 4.6							
131		± 7.8							
132		± 7.8							
133		± 4.7							
134		± 5							
135		± 4.2							
136		± 3.9							
137	1.63	43 ± 5.2	567 ± 4	42 55 58	8.0	−13.60	2.6	0.60	
138	1.39	45 ± 7.7	3614 ± 2	47 61 63	48.0	−15.86	82	2.40	
139	3.85	65 ± 2.9	1074 ± 3	60 80 83	14.9	−14.40	20	2.22	
140	3.22	57 ± 3.7	1290 ± 3	90 100 115	15.8	−15.25	20	1.03	
141	0.83	38 ± 4.9	569 ± 2	22 28 30	7.8	−12.03	0.85	0.84	
142		± 7							ATCA
143	6.2	98 ± 3.8	706 ± 2	66 80 85	11.2	−13.75	19	3.88	
144	8.41	187 ± 3.7	483 ± 1	45 60 64	6.3	−12.91	7.9	3.48	
145	3.1	6.1 ± 9	707 ± 4	50 73 78	11.2	−13.78	9.5	1.88	
146		± 4.1							
147	21.3	121 ± 23	3026 ± 3	173 284 288	37.1	−18.06	6.90	2.64	N
148	3.36	85 ± 3.6	602 ± 3	38 54 59	7.6	−13.46	4.6	1.21	
149	3.0	56 ± 4.2	407 ± 2	60 62 71	6.1	−14.10	2.7	0.39	
150		± 6.1							
151	2.71	69 ± 3.6	431 ± 8	33 35 70	6.5	−13.53	2.7	0.68	
VPC873		± 2.9							
152	2.33	72 ± 2.2	838 ± 3	34 43 45	11.4	−14.13	7.4	1.05	
N4523	20.54	194 ± 6.1	260 ± 2	120 134 139	2.6	−12.71	3.4	1.80	
I3517	1.81	29 ± 6.2	438 ± 3	74 106 108	4.7	−13.11	0.92	0.34	
I3521	0.38	11 ± 3.2	932 ± 8	34 44 50	11.1	−16.45	1.1	0.2	
153		± 4.9							
154	2.18	46 ± 5.4	455 ± 4	31 42 60	6.6	−13.53	2.3	0.56	
155		± 4.1							
156		± 4.7							
157		± 6							ATCA
158	0.66	26 ± 4.6	636 ± 2	27 33 34	9.1	−13.24	1.4	0.45	
159	1.83	38 ± 4.6	1822 ± 4	43 73 75	24.7	−14.66	26.0	2.28	
160	0.87	36 ± 4.7	299 ± 3	28 40 44	4.9	−11.53	0.51	0.80	
161	2.28	30 ± 3.1	1800 ± 5	72 82 88	26.3	−15.63	24	0.88	
162		± 4.5							
163		± 4.6							
164	9.04	214 ± 4.5	993 ± 2	30 47 50	11.9	−15.07	30	1.82	
165		± 3.7							
166		± 7.6							

kk 127: in spite of $v = 131$ km s^{-1} the galaxy looks distant
kk 129: undetected in HI (7)
kk 138: NGC 4295 ($v = 8568$ km s^{-1}) at $4'$, no confusing object to be seem
kk 146: heliocentric velocity 162 km s^{-1} (6)
kk 150: heliocentric velocity 468 km s^{-1} (6)
kk 155: heliocentric velocity 61 km s^{-1} (6)
kk 162: the object looks like an emulsion defect
kk 164: $v = 4660$ km s^{-1} (NED), NGC 4688 ($v = 987$ km s^{-1}) at $6.7'$ SW: confused

Table 2. continued

KK No.	HI-flux Jy km s^{-1}	$S_{\max}$ mJy	velocity km s^{-1}	line width km s^{-1}	distance Mpc	M_{Bt}	HI mass $10^7 M_\odot$	M_{HI}/L_B	Comments
1	2	3	4	5	6	7	8	9	10
167	1.99	51 ± 3.2	1247 ± 4	37 50 52	16.6	−14.55	13	1.24	
168	1.35	45 ± 4.3	2785 ± 4	39 41 54	35.8	−15.53	33	1.31	
169	1.65	39 ± 4.2	1818 ± 2	46 54 55	23.4	−14.88	20	1.40	
170	1.71	43 ± 4.3	641 ± 3	35 55 59	6.5	−12.57	1.7	1.04	
171		± 10							
172	2.0	43 ± 5.1	560 ± 3	53 64 66	6.6	−12.96	2.1	0.88	
173	2.58	74 ± 8.4	1015 ± 2	20 70 75					
U8091	8.78	310 ± 7	214 ± 1	27 38 41	2.2	-12.48	0.98	0.75	
174	8.76	9.2 ± 1	1905 ± 2	138 145 147	22.2	−16.19	100	2.18	ATCA
175	2.28	68 ± 4	701 ± 3	38 43 48	9.9	−13.00	5.3	2.15	
176	3.41	92 ± 5.0	828 ± 1	41 48 50	8.9	−12.62	6.2	3.58	
177		± 4.8							
178		± 7.2							
180		± 8							
181	3.64	45 ± 6.5	1930 ± 3	88 100 102	25.8	−14.86	60	4.39	
182	2.12	108 ± 6	613 ± 1	16 22 24	5.2	−12.78	1.3	0.66	ATCA
272		± 7							ATCA
183	2.23	29 ± 8.1	1573 ± 3	87 93 95	5.2	−10.75	1.4	4.53	
185		± 5.7							
186		± 9.8							
187	1.70	39 ± 5.9	2087 ± 6	38 80 85	25.3	−15.27	26	1.31	
188		± 8.5							
191	2.41	40 ± 6	368 ± 6	62 81 92	5.9	−10.71	2.0	6.69	
192	0.67	22 ± 5.8	1203 ± 9	27 37 40	16.8	−14.52	4.0	0.40	
193		± 4.4							
194		± 6							
195	5.5	200 ± 20	564 ± 4	21 27 30	4.9	−11.51	3.1	5.0	N
196		± 36							ATCA
198		± 32							N
199		± 7							
200	1.33	57 ± 8	485 ± 3	20 31 34	3.9	−11.62	0.51	0.74	
201		± 28							N
202		± 6.9							
204	5.6	95 ± 20	1463 ± 8	71 89 98	16.7	−16.50	37	0.60	N
205		± 4.3							
206	6.2	115 ± 9	588 ± 2	57 71 89	9	-15.43	12	0.51	
207		± 5							
208	36.2	878 ± 12	400 ± 2	36 59 65					
209		± 5.2							
210	6.4	100 ± 18	1650 ± 2	89 98 102	20.2	−15.31	62	2.97	N
212	1.07	23 ± 4.4	1241 ± 6	57 65 68	17.9	−15.44	9.0	0.39	
215		± 7							ATCA
216	5.30	90 ± 5.1	1355 ± 6	63 82 89	19.4	−16.77	50	0.63	
218		± 15							
219	0.85	17 ± 4.6	1276 ± 3	68 98 99	17.9	-14.15	6.4	0.90	

kk 170: HI detection by Matthewson & Gallagher (1995)
kk 174: $v = 1905$ km s^{-1} conflicts with the galaxy morphology
kk 177, 180: undetected in HI (7)
kk 191: NGC 5055 ($v = 510$ km s^{-1}, $W = 406$ km s^{-1}) at 24.1′ E, possible confusion through far sidelobe
kk 192: NGC 5033 ($v = 876$ km s^{-1}, $W = 452$ km s^{-1}) at 10.8′ W, different velocity range, no confusion
kk 205: undetected in HI (6)
kk 208: 20′ from NGC 5236, confusion with the extended HI-halo of M 83 (4)

Table 2. continued

KK	HI-flux	S_{max}	velocity	line width	distance	M_{Bt}	HI mass	M_{HI}/L_B	Comments
No.	Jy km s^{-1}	mJy	km s^{-1}	km s^{-1}	Mpc		$10^7 M_\odot$		
1	2	3	4	5	6	7	8	9	10
220	0.8	33 ± 5.6	769 ± 2	27 33 34	11.1	−13.76	2.3	0.47	
223	4.26	53 ± 5.5	2594 ± 8	69 130 138	35.8	−15.45	130	5.51	
224	0.84	25 ± 6.7	1156 ± 6	26 43 54	16.8	−14.49	5.3	0.55	
225		± 6.3							
226		± 7							ATCA
227		± 7.8							
228	1.55	41 ± 5.9	1972 ± 3	44 64 66	28.1	−15.68	30	1.02	
229	0.31	25 ± 3	1355 ± 1	14 21 24	15.3	-14.95	1.7	0.12	ATCA
230	1.87	113 ± 6.4	61 ± 1	20 29 32	1.9	−9.57	0.17	1.58	
274	6.3	57 ± 15	2598 ± 6	62 73 78	32.5	−16.06	160	3.79	N
231		± 7.1							
275	9.08	106 ± 5	1633 ± 3	122 148 153	19.2	−17.30	79	0.61	ATCA
232	0.86	24 ± 5.5	2960 ± 9	37 47 51	41.5	−16.11	36	0.83	
233	4.18	55 ± 4.5	724 ± 2	76 91 93	11.9	−14.60	14	1.26	
234		± 6							ATCA
236	5.18	20 ± 6	−150 ± 1	21 34 36					
237	5.22	174 ± 5.6	−177 ± 1	24 34 37					
238	2.03	32 ± 5.9	2435 ± 9	58 88 92	36.0	−16.22	64	1.34	
239		± 6							ATCA
240	5.2	30 ± 3	1371 ± 5	176 188 191	16.1	−17.55	13	0.08	ATCA
241	12.32	174 ± 8	1152 ± 3	65 90 84	13.2	−15.03	51	3.17	ATCA
242	2.03	44 ± 3	426 ± 6	100 118 133	9.1	−11.01	8	20.15	
243	2.17		957 ± 2	32 60 70	11.0	−14.18	6.8	0.78	
245		± 4							
246	8.3	149 ± 30	358 ± 3	53 60 71	5.4	−12.28	5.3	3.68	N
247		± 7							ATCA
249	18.8	68 ± 20	2089 ± 10	124 131 158	28.5	−17.09	360	2.93	N
250	20.0	244 ± 6	127 ± 2	90 104 107	5.6	−14.54	15	1.44	
251	14.62	223 ± 8	126 ± 2	64 87 94	5.6	−13.72	11	2.23	
252	1.36	45 ± 5	132 ± 3	27 47 50	5.6	−14.56	1.1	0.10	
253		± 7							ATCA
254		± 8							
255	1.16	63 ± 4	1682 ± 1	36 44 48	21.1	−15.45	12	0.52	ATCA
256		± 7							ATCA
257	3.36	70 ± 5	705 ± 1	77 80 84	8.8	−14.59	6.2	0.58	ATCA
258		± 32							N
259		± 7							ATCA
260		± 6							ATCA

kk 223: 6.5 arcmin NE of UGC 8726 ($v = 2334$ km s^{-1}), confused
kk 227: companion of NGC 5371
kk 236, 237: probably local HI
kk 242: near NGC 6503, no obvious confusing object within the antenna beam and 1st sidelobes
kk 245: resolved into stars with the 6-m telescope (SAO), $v = -157$ km s^{-1} (1)
kk 254: undetected in HI (3)
kk 260: near NGC 7531

1. Huchra J. (1995)
2. Gallagher J.S. et al. (1995).
3. Huchtmeier W.K. et al. (1997).
4. Huchtmeier W.K. et al. (1981).
5. Matthews L.D. et al. (1995).
6. Huchtmeier W.K. & Richter O.G. (1989b).
7. Schombert J.M. et al. (1992).